Behavioral/Systems/Cognitive

Integration of Vibrotactile Signals for Whisker-Related Perception in Rats Is Governed by Short Time Constants: Comparison of Neurometric and Psychometric Detection Performance

Maik C. Stüttgen[1,2] **and Cornelius Schwarz**[1,2]

[1]Werner Reichardt Centre for Integrative Neuroscience, and [2]Hertie Institute for Clinical Brain Research, University of Tübingen, Tübingen 72076, Germany

Rats explore environments by sweeping their whiskers across objects and surfaces. Both sensor movement and repetitive sweeping typical for this behavior require that vibrotactile signals are integrated over time. While temporal integration properties of neurons along the whisker somatosensory pathway have been studied extensively, the consequences for behavior are unknown. Here, we investigate the ability of head-fixed rats to integrate information over time for the detection of near-threshold pulsatile deflection sequences applied to a single whisker. Psychometric detection performance was assessed with whisker stimuli composed of different numbers of pulses (1-31) delivered at varying frequencies (10, 20, 100 Hz). Detection performance indeed improved with increasing number and frequency of pulses, albeit this improvement was much lower than predicted by probabilistic combination, suggesting highly sublinear integration of pulses. This behavioral observation was reflected in the firing properties of concomitantly recorded barrel cortex neurons, which showed substantial response adaptation to repetitive whisker deflection. To estimate the integration time with which barrel cortex neuronal activity must be read out to match behavior, we constructed a model monitoring spiking activity of simulated neuronal pools, where spike trains were channeled through a leaky integrator with exponential decay. Detection was accomplished by simple threshold crossings. This simple model gave an excellent match of neurometric and psychometric data at surprisingly small time constants τ of 5–8 ms, thus limiting integration largely to $<$25 ms. This result carries important implications regarding sensory processing for whisker-mediated perception.

Introduction

Signal detection performance of human and animal observers benefits from repetitive activation at perceptual threshold in several sensory systems ["temporal summation"; audition: Heil and Neubauer (2003); Zwislocki (1960); touch: Gescheider et al. (1999); Verrillo (1965)]. The neural processes underlying this phenomenon must involve some sort of temporal integration of incoming signals. Temporal integration can be loosely defined as an accumulation of evidence over time, and has been shown to hold close links to perception also in discrimination tasks: for example, signals ramping up with accumulating sensory evidence appear downstream of primary sensory areas during perceptual decision making (Shadlen and Newsome, 1996; Roitman and Shadlen, 2002).

When rats sweep their whiskers across objects or textures, the spatial pattern is converted into a high-speed whisker vibration (the "vibrotactile signal"), whose dynamics are represented faithfully by first-order neurons in the trigeminal ganglion (Jones et al., 2004). Since the vibrotactile signal varies over time, it seems necessary to perform some sort of temporal integration of signals to extract features that carry information about the spatial configurations being palpated. For instance, the assessment of spectral parameters of the vibration (e.g., central frequency), shown to carry texture-specific information (Hipp et al., 2006), requires such temporal integration of the vibrotactile signal. The same argument holds for vibrotactile signals composed of identical pulses delivered at different interpulse intervals, requiring e.g., a pulse-counting mechanism (Salinas et al., 2000). On the downside, temporal integration necessarily involves a loss of the fine-grained structure of the input.

The type of temporal integration needed to count pulses or to calculate intensity is some sort of summing the vibrotactile signal over time. In contrast to this expectation, neurons along the whisker-related tactile pathway show strong firing rate adaptation with repetitive deflections at frequencies higher than 10 Hz, indicating highly sublinear temporal integration (Fanselow and Nicolelis, 1999; Chung et al., 2002; Arabzadeh et al., 2003; Garabedian et al., 2003; Khatri and Simons, 2004; Sanchez-Jimenez et al., 2009). Adaptation is strongest in primary somatosensory cortex and seems to be at least partly based on the action

Received Aug. 12, 2009; revised Nov. 23, 2009; accepted Nov. 23, 2009.

This research was supported by a grant from the Deutsche Forschungsgemeinschaft (SFB 550-B11).

Correspondence should be addressed to Cornelius Schwarz, Hertie-Institute for Clinical Brain Research, Department of Cognitive Neurology, University of Tübingen, Otfried-Müller-Strasse 27, 72076 Tübingen, Germany. E-mail: cornelius.schwarz@uni-tuebingen.de.

M. C. Stüttgen's present address: Department of Biopsychology, Institute of Cognitive Neuroscience, Faculty of Psychology, GAFO 05/620, University of Bochum, Bochum, Germany.

DOI:10.1523/JNEUROSCI.3943-09.2010

 0270-6474/10/302060-10$15.00/0

of intracortical inhibitory networks (Butovas and Schwarz, 2003, 2006; Webber and Stanley, 2004). To explain how this feature can be aligned with the need to integrate the vibrotactile signal, the behavioral capacity for temporal integration has to be assessed as a benchmark against which to compare neural firing patterns. Such data has not been available so far.

To systematically assess how the whisker system makes use of temporal integration, we asked whether rats' detection performance of near-threshold repetitive whisker deflections (pulses) varies as a function of pulse number and interpulse interval. In a next step, we investigated the time constant with which barrel cortex neuronal activity has to be integrated to match the improvement of detectability observed behaviorally. We found that stages downstream of barrel cortex appear to use surprisingly short time constants. This finding provides the basis for the elucidation of temporal integration for whisker-mediated perception.

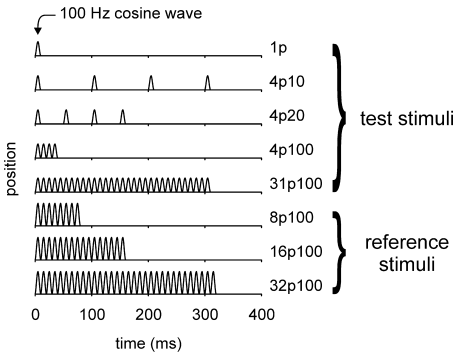

Figure 1. Schematic illustration of the whisker stimuli. Each stimulus consisted of one or more pulses delivered at varying frequencies for a variable duration. Each pulse consisted of a single cosine whisker deflection of 100 Hz. Reference stimuli are not drawn to scale; see methods for detailed stimulus description.

Materials and Methods

All experimental and surgical procedures were performed in accordance with the German Law for the Protection of Animals. Subjects were two female Sprague Dawley rats (Harlan Winkelmann), aged 12–16 weeks at the time of implantation.

Rats and surgery. Surgical procedures and the behavioral task have been described in detail before (Stüttgen et al., 2006; Stüttgen and Schwarz, 2008). Briefly, the rats were equipped with a dental cement head mount that was anchored to the skull with stainless steel screws. A mounting screw turned upside down was placed in the head mount for later fixation. During head mount surgery, a trepanation over the barrel cortex was performed. The C1 barrel was located by mapping the cortex with a single intracerebral electrode. A 2-by-3 multielectrode array (interelectrode distance, ~250–375 mm) was centered over the identified location of C1 and slowly inserted into the cortex and fixed to the head mount with dental cement. The wound was treated with antibiotic ointment and sutured. Analgesia and warmth were provided after surgery. Rats were allowed to recover for at least 14 d before habituation training. Rats were housed individually and kept under a 12/12 h light/dark cycle with water and food available *ad libitum* except during behavioral testing, when the rats were water-restricted for 5 d per week. Drops in body weight, monitored daily, were prevented by supplementary water.

Electrophysiology. The movable multielectrode arrays contained glass-coated, pulled and ground platinum tungsten electrodes (impedance 2–6 MΩ; Thomas Recording) manufactured in our laboratory. Electrode depth could be adjusted by turning a small screw (250 μm per revolution). After each successful recording session, we lowered the electrode by a quarter to half revolution. Voltage traces picked up by the electrodes were bandpass-filtered (200–5000 Hz) and recorded at a sampling rate of 20 kHz using a multichannel extracellular amplifier (Multi Channel Systems). Spikes were detected offline using amplitude thresholds. Two-millisecond cutouts centered on the time bin in which the voltage trace first traversed the amplitude threshold were recorded and sorted using a custom-written software package (Hermle et al., 2004). Artifacts were removed and neurons sorted to yield either single- or multiunit spike trains (SU and MU, respectively).

Behavioral task and whisker stimulation. Rats were trained on a Go-/No-Go detection paradigm. The animals' task was to respond to whisker deflections occurring on average every 5 s (±2.5 s, uniform distribution) by licking from a water spout. If they emitted a lick response within 600 ms after stimulus onset (the window of opportunity), they received a droplet of water as positive reinforcement. To discourage random licking during the intertrial interval, presentation of a new stimulus was delayed by 5 s (±2.5 s) in case the rat licked during the prestimulus period. Premature responses (licks occurring within the first 75 ms of the window of opportunity) led to trial break-off without reward delivery. Both premature responses as well as responses to catch trials (see below) led to mild punishment (presentation of a bright light for 1 s).

Whisker stimuli were delivered using piezoelectric actuators, deflecting the C1 whisker ~5 mm from the whisker base. Command voltages were generated in LabVIEW 8 (National Instruments) and delivered at 100 kHz. Near-threshold stimuli consisted of short pulses fixed in amplitude and frequency (100 Hz cosine waves; amplitude was adapted for each rat such that a single pulse was detected on average in ~50% of cases (rat 1: ~70 μm with peak velocity of ~25 mm/s in either direction, rat 2: ~30 μm with peak velocity ~10 mm/s) (see Fig. 1 for a sketch of the stimulus waveforms; reference stimuli not to scale). Stimuli differed with regard to number of pulses (1, 4, or 31) and pulse frequency (10, 20, or 100 Hz). In addition to the five test stimuli (from here on referred to as 1p, 4p10, 4p20, 4p100, and 31p100, with the first number denoting number of pulses p, and the second number denoting presentation frequency), we included "catch trials" in which no stimulus was presented but randomly occurring licks were registered to arrive at a measure of chance performance (i.e., hits without stimulus-guided decisions). To maintain the animals' motivation throughout an experimental session comprising up to 250 trials, we additionally included three suprathreshold reference stimuli, consisting of 8, 16, or 32 100 Hz pulses having large amplitudes (~250 μm) and high velocities (>60 mm/s in both rostral and caudal directions), delivered at 100 Hz.

Stimulus types were presented in a pseudorandom sequence: the nine stimulus types—five test stimuli, three reference stimuli and the null (catch) stimulus—were presented once each in random sequence before one of them was presented again. Each stimulus was presented for on average 20 times (range 15–25).

The animals were not explicitly trained not to move their whiskers during the task. However, previous EMG recordings in a similar task (Stüttgen et al., 2006) as well as video observation during task performance indicated that whisker movements around the time point of stimulus application are almost completely absent.

Modeling. To systematically investigate whether behavioral performance could be realized by monitoring the integral of past firing in a population of neurons, we constructed a model based on Monte-Carlo simulations of spike trains, with spiking probabilities derived from the 22 single units' spike trains in our dataset (see Fig. 5 for an outline of the model). For each neuron and each stimulus type, we first calculated spiking probability in consecutive 1 ms bins as a function of time as given by the recorded data (±1000 ms relative to stimulus onset), yielding a simple peristimulus time histogram for each stimulus for each single unit, scaled in units of "spike probability" per 1 ms bin. Next, we selected the m units with the highest signal-to-noise ratio (SNR), where m could take the values {5,10,20}. A neuron's SNR was determined by calculating Glass's Δ (see below) for single-pulse spike probabilities relative to spontaneous activity. We then constructed neuronal pools that included these m neurons, with pool sizes taking one of n values, where n always was a member of the set {5, 10, 20, 40, 100, 200, 500}. We only considered models in which n was an integer multiple of m (see Fig. 5, "Data base"). For reasons of mathematical convenience, we took only the 20 most sensitive neurons from the 22 neurons available. The remaining two neurons were not qualitatively different from the others in any obvious way.

We constructed a 2-s-long random spike train for each of the n neurons as given by the neuron's peristimulus time histograms (PSTHs); in cases where $n > m$, neurons were cloned to contribute additional random spike trains. We then summed spike trains over all n neurons to yield a "population PSTH" for a single presentation of a stimulus. Thus, population PSTH refers to the summed spike counts of n simulated spike trains, where each spike train is generated by randomly assigning spikes to 1 ms bins, where the probability of a spike occurring in an individual bin is determined by the respective unit's original PSTH (see Fig. 5, "Pooling"). To assess the role of temporal integration, population PSTHs were convolved with an exponential decay function (of the form $\exp(-t/\tau)$, normalized to have an integral of unity), where t is time and τ is the time constant of the function), with τ being a member of the set {0.2, 0.5, 1, 2, 5, 8, 10, 15, 20, 35, 50} in units of milliseconds (see Fig. 5, "Integration").

This procedure was repeated 1000 times, yielding 1000 filtered population PSTHs for each stimulus. The model should base its decision about the presence or absence of a signal on the peak spike counts in the filtered population PSTHs. To arrive at a meaningful criterion, we determined the 54th percentile of peak spike counts in the population PSTHs to the single-pulse stimulus between 0 and 200 ms after stimulus onset. This results in 46% of the 1000 population PSTHs exceeding threshold, which compares well with the 46% catch-corrected response rate observed with our rats (compare Figs. 2*a*, 5, "Calibration").

Catch-corrected hit rates were calculated using the following equation:

$$HR_{c,i} = \frac{HR_i - FA}{1 - FA}, \qquad (1)$$

where $HR_{c,i}$ is the catch-corrected hit rate for stimulus i, HR_i is the obtained hit rate for stimulus i, and FA is the false-alarm rate [i.e., response rate to the catch stimulus (Blackwell, 1952)]. The reason for applying this formula is that a fraction of the rats' responses to near-threshold stimuli presumably resulted from "guessing," i.e., emitting random licks without the presence of a sensation. This fraction can be estimated by using the false-alarm rate as shown in Equation 1. Since we were only interested to model 'true' detections from barrel cortex neuronal activity, we calibrated the spiking threshold to the corrected hit rate for the single pulse stimulus. Similarly, the model's fit to the behavioral data was evaluated on the basis of corrected hit rates, too. However, in a variation of the modeling exercise we used uncorrected hit rates and found the results to be highly similar.

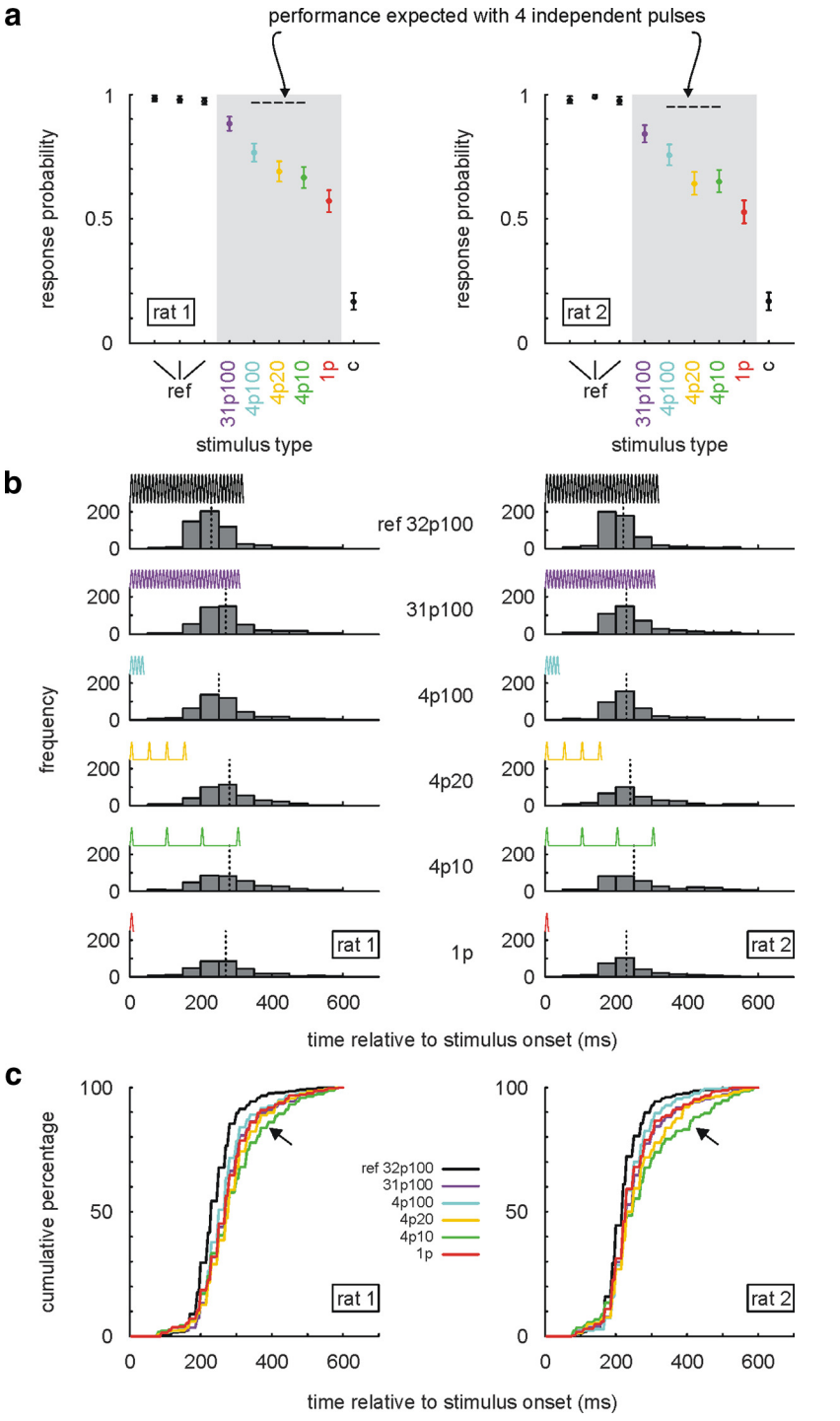

Figure 2. Behavioral results. ***a***, Overall response probability for both rats (left, rat 1; right, rat 2) pooled across all sessions, plotted with binomial CI95. Each data point is based on 400–500 trials. Dashed lines above four-pulse stimuli depict performance expectation based on probability summation (see Results). Gray shading highlights the five test stimuli (see Materials and Methods). ***b***, Histograms of reaction times for each of the five test stimuli. Broken vertical lines indicate median reaction times. Stimulus traces superimposed for clarity; reference stimulus trace amplitude not to scale. Left, Data from rat 1; right, data from rat 2. ***c***, Cumulative frequency distributions of reaction times, separated by stimulus type. Arrows highlight increased frequency of long reaction times for the four-pulse stimulus at 10 Hz. Left, Data from rat 1; right, data from rat 2.

The spiking threshold was applied to the population PSTHs of all other stimuli. The detection rate for a given stimulus (or false alarm rate in case of catch) was then equal to the fraction of PSTHs exceeding the derived threshold (see Fig. 5, "Model response rates and RT").

The reaction times of the model were calculated by taking the times at which the simulated neuronal responses first surpassed the threshold ("detection time") within each population PSTH, and then adding to each detection time all reaction times to the 1p stimulus obtained from each rat. The resulting reaction time distributions were transformed into percentiles for comparability to each other and the rats' distributions.

Importantly, peak spike counts in the population PSTHs were only extracted for the interval −450 to +500 ms relative to stimulus onset.

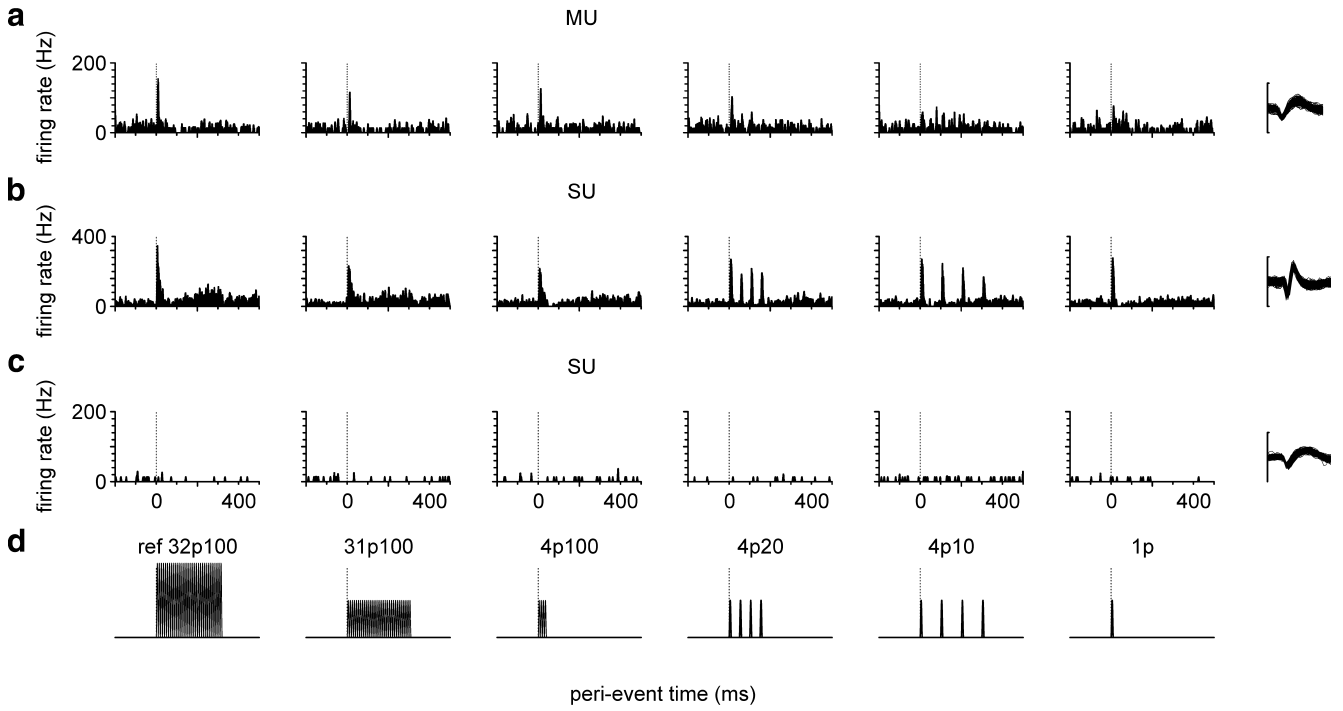

Figure 3. PSTHs for three example units recorded from barrel cortex, bin width 1 ms, traces smoothed with a Gaussian kernel of 1.5 ms width (***a–c***). Right, 200 overlaid example waveforms for each example unit (scale bar, 400 μV). ***d***, Stimulus waveforms corresponding to PSTH panels are depicted for clarity in the bottom row; reference stimulus not to scale.

This interval was chosen because we reasoned that to emit a response in the interval 75–600 ms after stimulus onset (as required in our behavioral paradigm), the sensory event leading to the response had to be between 75 ms minus the maximum reaction time observed, and 600 ms minus the minimum reaction time observed. Maximum and minimum reaction times were taken from actually measured reaction time distributions for the single-pulse stimulus and set to be 525 and 100 ms, respectively (see also Fig. 2*b*).

As noted above, this simulation was run using time constants τ ranging from 0.2 to 50 ms. The time constant represents the time it takes a system's initial response magnitude to drop to ~63% of its maximum at time 0. After three time constants, the function reaches a value <4% of its maximum; with five time constants, this number decreases to 1%.

Goodness of fit of response rate distributions (model vs rats) was evaluated using the coefficient of determination (r^2). To compare the model's and the rats' reaction time distributions, we constructed a "similarity index": first, we reduced every reaction time distributions to its percentiles. Then, we calculated the percentile-wise difference in reaction times for each multipulse test stimulus from the single-pulse stimulus (i.e., 31p100, 4p100, 4p20, 4p10 vs 1p), yielding "difference vectors" composed of 100 elements each. This was done for both rats and each model at each value of τ. The difference between the rats' and the model's difference vectors was calculated and squared, the four resulting vectors (measuring dissimilarity) were averaged, and their reciprocal was logarithmized. Thus, larger values of the similarity index indicate higher similarity of the distributions, with 0 occurring in the case of identity.

Statistics. Statistical analyses used in this study included repeated-measures ANOVA (rmANOVA), paired *t* tests, and the construction of 95% confidence intervals (CI95). CI95s were generally constructed from *t*-distributions or, in the case of proportions, from binomial distributions (Clopper–Pearson method).

We used three effect size measures to complement *p* values (Kline, 2004). Hedge's *g* is a widely used effect size indicator that expresses the difference between the means of two groups in units of the pooled SD, as follows:

$$g = \frac{\text{mean}_{\text{group A}} - \text{mean}_{\text{group B}}}{\sqrt{\frac{\text{var}_{\text{group A}} + \text{var}_{\text{group B}}}{2}}}. \quad (2)$$

By convention, values of Hedge's *g* of 0.2, 0.5, and 0.8 are regarded as small, medium, and large, respectively.

For calculating neuronal SNR, we used a variant of Hedge's g called Glass's Δ. Δ is identical to *g* with the exception that the denominator represents the SD of the control group only (here: spontaneous activity), rather than a pooled estimate of the SD as in *g*.

For ANOVA, we used η squared (η^2), computed as follows:

$$\eta^2 = \frac{\text{SS}_{\text{effect}}}{\text{SS}_{\text{total}}}, \quad (3)$$

where $\text{SS}_{\text{effect}}$ is the sum of squared deviations of all group means from the grand mean multiplied by the number of observations, and SS_{total} is the sum of the squared differences between all individual scores and the grand mean. η^2 ranges from 0 to 1 and indicates what fraction of the overall variance of the dependent variable is explained by variation of a single independent variable. Its interpretation is therefore identical to that of the coefficient of determination, r^2. By convention, values of 0.1, 0.25, and 0.4 are regarded as small, medium, and large, respectively (Cohen, 1992). A value of 1 indicates that the entire variance in the data is explained by variations in the independent variable.

All data analyses were performed in MATLAB 7 (The MathWorks).

Results

Behavior

Figure 2*a* plots detection probability as a function of stimulus type, separately for each rat. For both rats, response probability ranged from ~0.17 for the catch stimulus to almost 1 for the three reference stimuli, exemplifying the adequacy of our Go/No-Go detection task: throughout experimental sessions, rats responded steadily to suprathreshold reference stimuli, and displayed low but measurable false alarm rates, such that detectability of near-threshold stimuli could be reliably assessed.

Inspection of Figure 2*a* reveals that the rat whisker system is indeed capable of temporal summation at detection threshold (shaded area): detection probability increased from the single-pulse stimulus to four-pulse stimuli to the 31-pulse stimulus, and did so for both rats by about the same amount (maximally ~0.3

increase in detection probability from single pulse to longest pulse train; rat 1: $F_{(4,29)} = 38.7$, $p < 10^{-16}$; rat 2: $F_{(4,29)} = 39.3$, $p < 10^{-16}$, rmANOVA). The observed pattern of stimulus detectability is highly consistent across rats – four pulses were consistently detected better than one pulse, 31 pulses were consistently better detected than four pulses (rat 1: t values from 3.5 to 11.4, all p values <0.005; rat 2: t values from 2.9 to 10.1, all p values <0.01; all df = 29).

If each additional pulse in a train conveys as much information as the first pulse [i.e., "probability summation" wherein detection probability for single pulses ($p_{\text{detect\_pulse}}$) is constant throughout the pulse train (Gescheider et al., 1999)], the resulting detection probability for trains containing n pulses is given by the following:

$$p_{\text{detect\_train}} = 1 - (1 - p_{\text{detect\_pulse}})^n. \quad (4)$$

Using Equation 4, we calculated the expected response probability for trains of four pulses (Fig. 2*a*, horizontal dashed lines), and found that the actually observed response rates fell well short of this expectation for all three stimuli. Another prediction of probability summation is that response probabilities for multipulse stimuli should not depend on the frequency with which they are applied. The data in Figure 2*a* are clearly at odds with this prediction as well: both rats detected four pulses delivered at 100 Hz better than when applied either at 10 Hz or 20 Hz (rat 1: $t_{(29)} = 2.4$ and 3.9, p values <0.05; rat 2: $t_{(29)} = 4.8$ and 4.9, p values $<10^{-4}$). Response rates to four pulses at 10 Hz and 20 Hz, however, did not differ significantly from each other (rat 1: $t_{(29)} = 1.3$, CI95 for difference: −0.09 to 0.02; rat 2: $t_{(29)} = 0.6$, CI95 for difference: −0.04 to 0.08). Also, average response rates to 31 pulses at 100 Hz were only mildly increased relative to four pulses delivered at the same frequency (rat 1: 0.12, CI95 for difference: 0.08 to 0.16; rat 2: 0.8, CI95 for difference: 0.04 to 0.13; prediction from probability summation ~0.25 for both rats). Together, these results speak against the operation of probability summation: increasing the number of pulses from one to four confers less increase of detectability than expected, and this advantage is dependent on pulse frequency.

Intuitively, one would expect to see the temporal summation effect—better detectability for longer pulse trains—also in prolonged reaction times. However, since the (uncorrected) response rate to the single-pulse stimulus was ~55% already, and the response rate was only mildly increased by applying multipulse stimuli (by ~0.1–0.3), a considerable fraction of the multipulse responses presumably originated from detection of the first pulse. Accordingly, only small differences in average reaction times may be expected. Indeed, reaction time distributions are hardly affected by stimulus type (Fig. 2*b*) [Hedge's g ranging from 0.05 to 0.27 (rat 1) and 0.06 to 0.33 (rat 2), amounting to <50 ms for all possible differences from the mean of the single-pulse response time distribution].

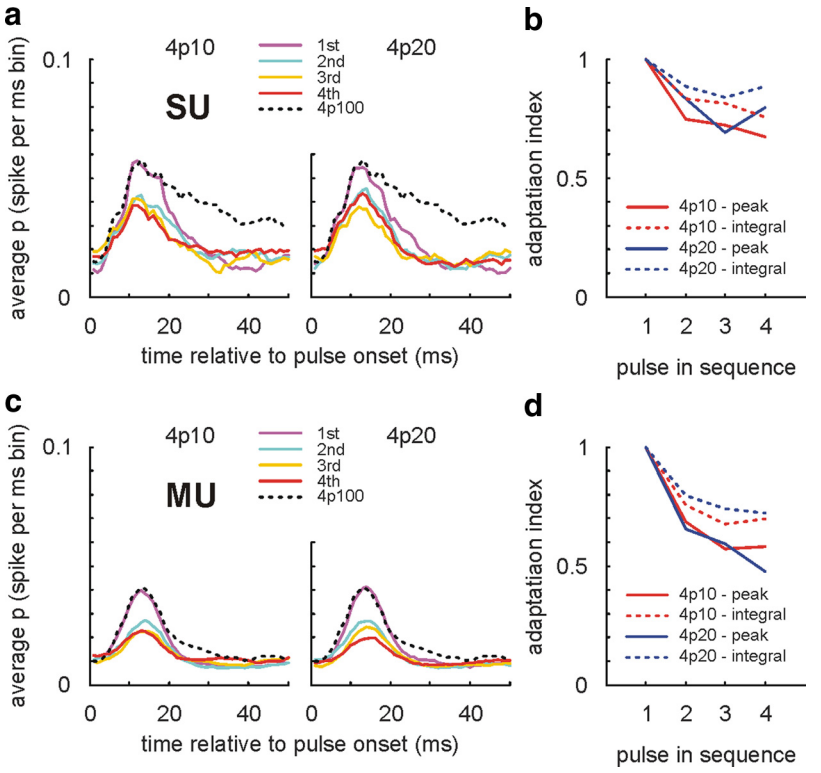

Figure 4. ***a***, Dynamics of adaptation, averaged over all single units ($n = 22$). Spike probability is plotted for 50 ms windows, smoothed with a boxcar filter of width = 10 ms (resolution: 1 ms). PSTHs are aligned to onset of each consecutive pulse. Left, Four pulses at 10 Hz; right, four pulses at 20 Hz. Black dotted line in both panels denotes four pulses at 100 Hz; here, the response to individual pulses could not be disentangled. ***b***, Adaptation index (AI), computed separately for maximum spike probability and spike count, shown for both stimuli. ***c***, ***d***, same as ***a***, ***b***, but for multi units ($n = 160$).

However, despite the small effect on the means, cumulative distributions of reaction times revealed the presence of heavy tails, which indicate an overrepresentation of long reaction times for the two long-lasting four-pulse stimuli (duration 160 and 310 ms for four pulses at 20 and 10 Hz, respectively) relative to two shorter stimuli (single-pulse and 4 pulses at 100 Hz): 90% of responses were registered within 370 ms (rat 1) and 360 ms (rat 2) for the single-pulse stimulus and 440 ms (rat 1) and 470 ms (rat 2) for the four-pulse stimulus at 10 Hz, a difference of 70 and 110 ms, respectively (Fig. 2*c*) [compare green, yellow, and cyan lines (4p10 and 4p20, respectively) to red lines (1p)].

In general, reaction times to all stimuli were surprisingly short, with medians ranging from 200 to 300 ms. Moreover, for the stimulus showing the strongest temporal summation effect (31 pulses at 100 Hz, equating a total stimulus duration of 310 ms) >75% of reaction times were <300 ms. This means that most of the responses were completed before this stimulus was over. Assuming an average response latency of ~250 ms from registration of a stimulus until the tongue has contacted the spout (seen with single pulses), this allows the rat to integrate, on average, over maximally 50–100 ms before issuing a response. On the other hand, reaction times permitting integration over the whole duration of the stimulus (300 ms + 250 ms response latency) were virtually absent (463/470, <1.5% of cases for rat 1, 424/428, <1% of cases for rat 2).

In summary, the behavioral data demonstrate (1) the existence of temporal summation, (2) a strong attenuation of the effects of additional pulses relative to the first pulse, (3) the implausibility of a simple probability summation as the mechanism underlying the summation effect, and (4) a weak temporal inte-

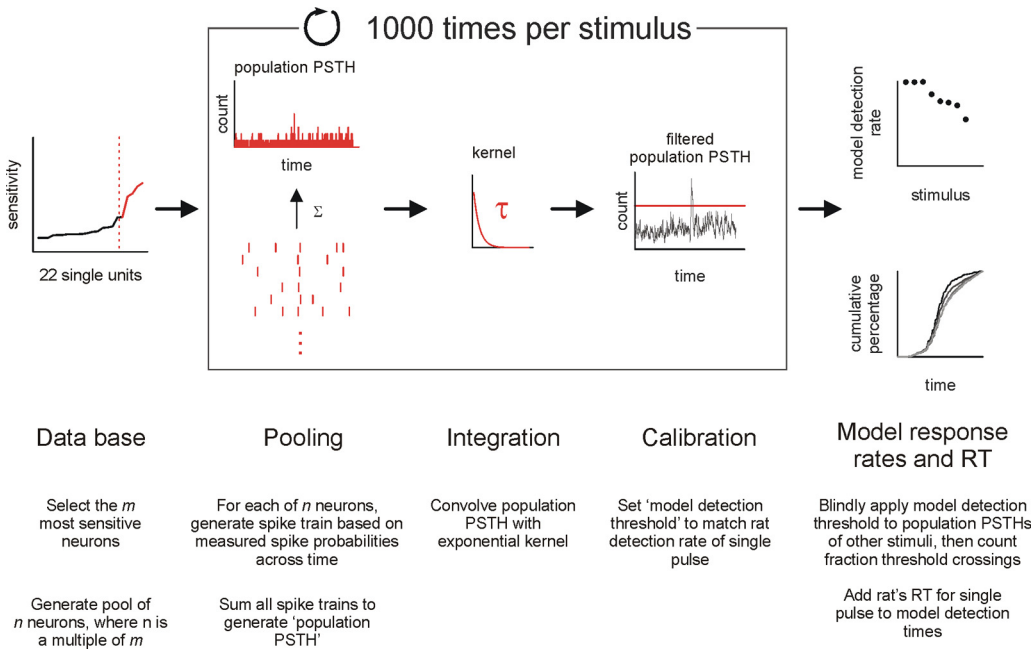

Figure 5. Outline of the probabilistic model. RT is reaction time. See Materials and Methods for details.

gration of neuronal responses that is limited to perhaps the initial 50–100 ms of a stimulus. In the next section, we will analyze responses recorded from barrel cortex while the rats performed the detection task.

Neurophysiology

Overall, we recorded a total of 22 single and 160 multi units (rat 1: 9 SU, 73 MU; rat 2: 13 SU, 87 MU; total: 182 units). Figure 3 shows several exemplary units' peristimulus time histograms (PSTHs) for the five test stimuli, as well as one reference stimulus for comparison. Figure 3*b* shows a single unit which provided a faithful reproduction of stimulus dynamics (compare the PSTHs for the two four-pulse stimuli delivered at 10 and 20 Hz with the stimulus waveforms in Fig. 3*d*). The multi unit in Figure 3*a* showed an excitatory response to stimulus onset only, while the single unit depicted in Figure 3*c* was not affected by the stimuli at all.

Qualitative inspection of these example units suggested that, indeed, subsequent pulses yield attenuated spike responses, concordant with the behavioral result that subsequent pulses provided only a minor aid in stimulus detection. Accordingly, we quantified neuronal response adaptation. Figure 4, *a* and *b*, plot adaptation characteristics separately for single and multi units, respectively. Figure 4, *a* and *c*, display average spike probabilities across single and multi units, respectively, for the four pulses delivered at 10 and 20 Hz (colored). For comparison purposes, the black dotted line plots the spike probability for the four pulses delivered at 100 Hz; since the spike responses to subsequent stimuli completely overlapped in this case, it was not possible to disentangle the spike responses in a pulse-wise manner. The plots reveal that, for both 10 and 20 Hz, responses to subsequent pulses were reduced. We quantified the amount of reduction using the adaptation index (AI) used in the study by Khatri et al. (2004). AI was computed in two ways: first, as the maximum spike probability within each 25 ms interval following pulse onset normalized to the maximum spike probability for the first pulse; second, as the integral of the spike probability (i.e., total spike count) in the same period, normalized in an analogous way. Figure 4, *b* and *d*, presents AI as a function of pulse number across single and multi units. Both maximum spike probabilities and spike counts progressively adapted, with the major amount of attenuation being achieved with the second pulse already. These results are in both qualitative and quantitative agreement with a previous report using suprathreshold stimuli in anesthetized rats (Khatri et al., 2004).

As an initial check whether the temporal summation effect seen in the behavior is mirrored by barrel cortex neuronal activity, we asked whether total spike count or peak firing rate within 350 ms after stimulus onset was affected by stimulus type across both single and multi units.

Firing rates were extracted from PSTHs smoothed by a low-pass Butterworth filter (cutoff frequency, 40 Hz). While both peak firing rate and total spike count were influenced by stimulus type, the observed differences between stimuli were extremely small ($\eta^2 < 0.01$ for both spike counts and peak firing rates for both rats). Also, mean and median spike counts and peak firing rates did not show the same ranking of stimulus types as that seen in behavior. In summary, averaged spike counts and peak firing rates were hardly affected by increasing stimulus duration or pulse number. In any case, the usage of a 350 ms window for the measurement of the response is likely to be inappropriate, given that the rats' reaction times hinted at integration times way shorter than 350 ms.

Modeling

To elucidate the mechanisms of temporal integration needed to match the neuronal sensitivities to that of the rat observers, we ran a Monte Carlo simulation that used exponential integration windows (see Fig. 5 for an outline of the modeling procedure and methods for details). Our model was meant to answer the question "how do downstream brain areas integrate barrel cortex signals to generate a decision about the presence or absence of a signal?". We reasoned that these downstream areas integrate barrel cortex output and apply a simple activity threshold to the resulting signal. To simulate this process, we took our single units' PSTHs and scaled it in terms of spike probability as a func-

tion of peristimulus time. Then, we constructed pools of 5, 10, 20, 40, or 100 artificial neuron that were composed of the 5, 10, or 20 most sensitive neurons in our sample. The reason we varied composition and size of the pool was to see whether different pools yield different best-matching time constants.

Each pool of neurons was presented with all stimuli, and the spike trains of all neurons in a pool were summed to generate a population PSTH, which was subsequently convolved with an exponential kernel with a specific time constant (we investigated time constants ranging from 0.2 to 50 ms). The model based its decision to report or not report a signal on simple threshold crossings of the population PSTH.

Figure 6*a* shows the resulting detection rate from a simulation with an integration time constant of $\tau = 5$ ms, generated by a pool composed of the 20 best neurons with a pool size of 40 (thus, in this combination, each neuron entered the pool twice). Comparison with Figure 2*a* highlights the similarity of the model's response rate patterns to that for both rats. Figure 6*b* shows this more explicitly by plotting the model's against the rats' response rates. For both rats, the match between model and behavior was excellent (both $r^2 > 0.97$).

If performance of the rats was based on monitoring population spiking activity over time and issuing a response if detection ensues, the model should predict the observed differences in reaction time between stimuli (Fig. 2*c*). To test this, we first determined the model's "detection times," i.e., the time points at which the spike count of each population PSTH exceeded its threshold. For $\tau = 5$ ms, detection times are plotted in Figure 6*c*. Detection times were almost exclusively found in the 25 ms bins beginning after pulse onset, with the first pulse of multipulse series yielding the most detection times. Intuitively, this concurs with our behavioral observation, detailed above, that detection was governed largely by the first pulse in each series. Also, detection time distributions for 4p10 and 4p20 show some additional peaks right after each additional pulse (Fig. 6*c*, arrows).

To see whether the model could also successfully account for the observed reaction time patterns (Fig. 2*c*), we calculated "model reaction times." These were constructed, in simple terms, by adding the model detection times to the rats' reaction times to the single pulse stimulus (see Materials and Methods for details).

Figure 6*d* shows cumulative model reaction time distributions, separately for reaction times taken from rat 1 and rat 2. The overall shape of the distributions resembles those of both rats rather well (minimum r^2 between percentiles of original and model distributions across all stimuli: 0.95). Moreover, the model reproduced the heavy tails of the distributions for two longest test pulse stimuli [4p10 and 4p20 (arrow); compare to Fig. 2*c*].

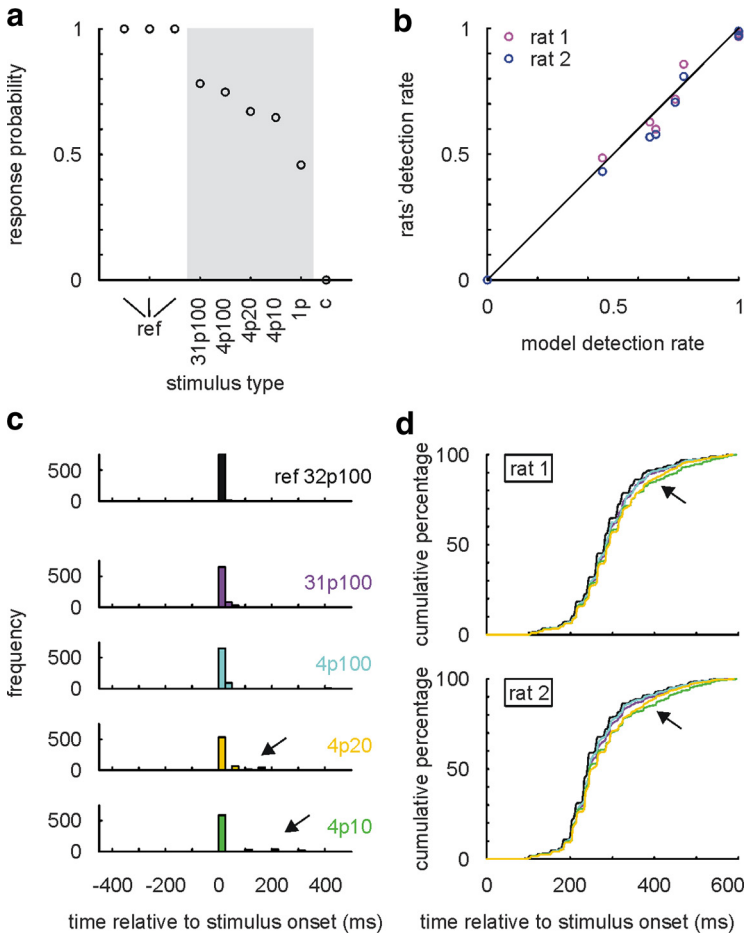

Figure 6. Model performance with a pool size of 40, composed of the 20 most sensitive neurons, at $\tau = 5$ ms. ***a***, Model detection rate as a function of stimulus type. Gray shading highlights the five test stimuli. ***b***, Scatterplot showing the high correlation between modeled and observed response rates, separately for rats 1 and 2. Black line represents unity. ***c***, Histograms showing the temporal distributions of model detection times, separately for each stimulus type. Bin width is 25 ms. Arrows point at late instances of detection to occur in the time bins right after stimulus delivery. ***d***, Cumulative frequency distributions of model reaction times, separately for each stimulus type and for reaction times taken from rat 1 (upper panel) and rat 2 (lower panel). Color code as in ***c***.

The match between psychometric and neurometric detection performance depended strongly on the value of τ, as well as the size but not the composition of the neuronal pool. Figure 7*a* shows the range of the 22 single units' SNR with bootstrapped 95% confidence intervals. Figure 7*b* shows goodness of fit (r^2 calculated between the model's and the rats' detection rates (compare Fig. 6*b*), averaged across rats) color-coded as a function of the three parameters. While the composition of the neuronal pool—the average sensitivity of its constituent neurons—did not have a marked influence, both pool size and τ did: larger time constants ($\tau \geq 35$ ms) yielded worse fits than smaller ones, and larger pools ($\geq$100 neurons) yielded worse fits than smaller pools.

Since we were mainly interested in temporal integration, we asked whether there is any range of values for τ that explain behavioral performance well, regardless of a neuronal pool's size or composition. Figure 7*c* (lower panel) plots the frequency of best τ values over all considered models. Strikingly, virtually all combinations of pool size and pool composition had their optimal τ values at either 5 or 8 ms.

To see whether this result holds for reaction times as well, we calculated a similarity index between the model's and the rat's reaction time distributions (see Materials and Methods). Inspection of Figure 7*d* reveals that, again, larger time constants yielded

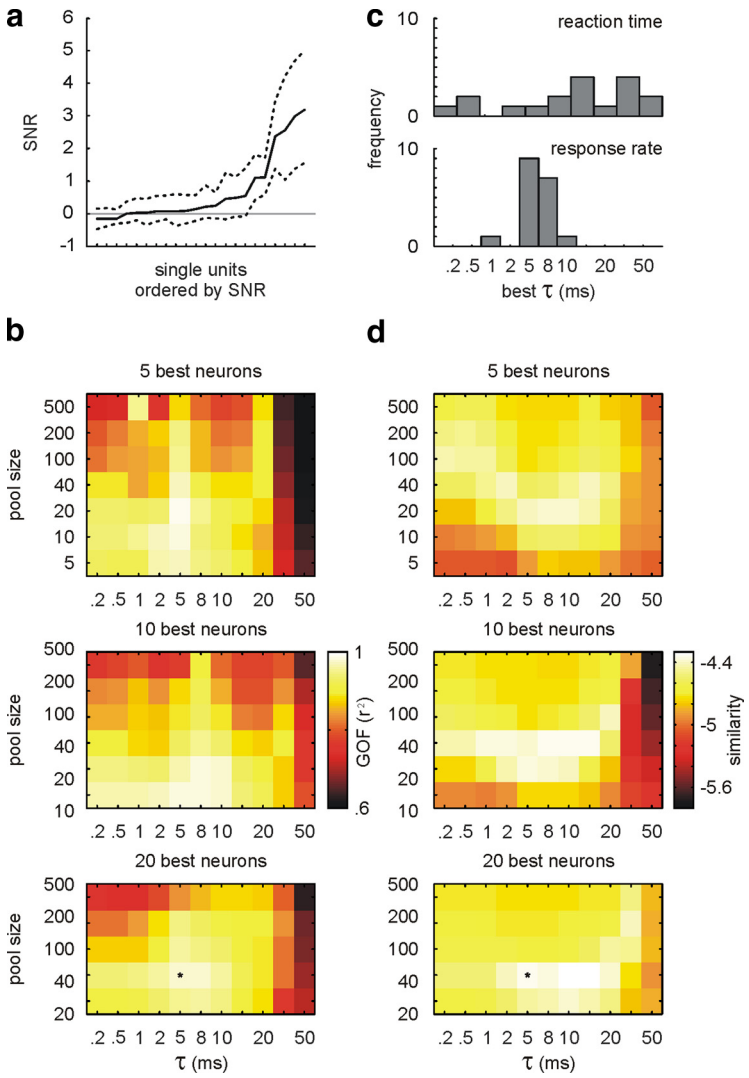

Figure 7. Dependence of model performance on τ. ***a***, SNR for 22 single units, ordered from low to high, with bootstrapped CI95 (broken lines). ***b***, Goodness of fit (GOF, measured as r^2) for response rate as a joint function of τ and pool size, separately for three pool compositions (subpanels). ***c***, Frequency distributions of best τ values, with all models considered. Upper panel, Reaction time fits; lower panel, response rate fits. ***d***, Same as ***b***, but for similarity of reaction time distributions. Asterisks denote the overall best model whose characteristics are depicted in Figure 6.

worse matches than short ones, consistently for variations in both pool size and pool composition. However, the distribution of optimal τ was broader than the one observed with response rate (Fig. 7*c*, upper panel, compare with lower panel).

To see which values of τ yielded the best fits when response rate and reaction time were considered simultaneously, we normalized both r^2 and our similarity index, and averaged these values for each model. Figure 8*a* reveals that the pattern derived from the separate consideration of both measures is replicated—small values of τ and smaller neuronal pools yield the best matches. In addition, we find that each subpanel has a "hot spot" of goodness of fit at intermediate values of τ. As Figure 8*b* shows, joint consideration of response rate and reaction time supports the optimal values of τ derived from response rate alone, with the vast majority of models featuring a τ of either 5 or 8 ms. The best model turned out to be a pool of 40 neurons, composed of the 20 most sensitive units in our sample, at an integration constant of 5 ms. This is the model whose performance is depicted in Figure 6.

Interestingly, virtually all tested models showed considerably better detection performance than the rat with increasingly longer time constants, with detection being almost 100% for most stimuli at time constants of 50 ms or longer. Thus, long integration times would actually serve to improve detection performance.

Together, a model monitoring coincident spiking in a small pool of neurons in barrel cortex is sufficient to explain both detection performance and variations in reaction time. Examination of different integration time constants suggests that rats could base their perceptual decision on strong but transient bursts of neuronal activity, integrated using a τ of 5–8 ms. This conclusion is valid over a vast range of pooling methods.

Discussion

This study set out to assess psychometric and neurometric variables to find out if (and how) the rat's whisker system integrates vibrotactile signals over time to improve detection. Behaviorally, we found that rats' detection benefited from series of pulses, but the summation was highly sublinear—far below what would be expected from statistical independence of single pulse detection. On the level of the cortex, neurons showed a highly integrated pattern of activity, with strong response to the first pulse and suppressed responses to the following pulses, with the degree of suppression depending on frequency. To match neurometric and psychometric performance, barrel cortical signals needed to be filtered by a leaky, exponential integrator with a short time constant of 5–8 ms, limiting the total integration time to <25 ms (i.e., 95% of integration achieved using a time constant of 8 ms).

A central premise of comparing neurometric and psychometric data is that the neurometric data are indeed relevant to execution of the psychophysical task. Hutson and Masterton (1986) reported the puzzling finding that lesions of the barrel field in primary somatosensory cortex had virtually no effect on the rats' abilities to perform a whisker-mediated vibrotactile discrimination task. This finding poses a problem for every study investigating the contribution of barrel cortex to whisker-mediated detection and discrimination abilities. However, there are some notable differences between their study and ours. These authors used classical delay-conditioning ("condition suppression technique"), where the conditioned stimulus (CS; change in whisker vibration frequency) and unconditioned stimulus (US; electric shock) are temporally contiguous, whereas we used an operant trace-conditioning paradigm, where CS (whisker deflection) and US (water delivery) are separated by a temporal gap, and the US is only delivered contingent on an operant lick response. Trace conditioning is certainly the more demanding task, as it requires the brain to store the "trace" of the CS until delivery of the US. In fact, there is ample evidence to indicate that the brain structures necessary for delay conditioning (mainly cere-

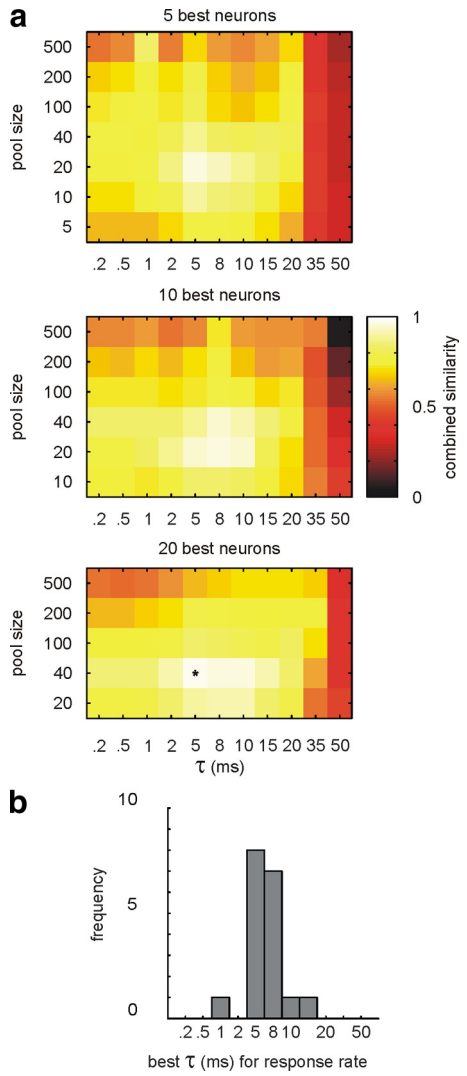

Figure 8. ***a***, Combined goodness of fit for response rate and reaction time as a function of τ, pool size, and pool composition. Asterisk, Overall best model. ***b***, Frequency distribution of best τ values, with all models considered.

bellum) are different from those necessary for trace conditioning [mainly hippocampus; for example, see the study by Clark and Squire (1998)]. Also, Galvez et al. (2007) showed that both acquisition and retention of a conditioned response in trace conditioning with whisker vibration as the CS require an intact barrel cortex, albeit this study was done in rabbits. Finally, settling this issue will require temporary lesions of barrel cortex during the execution of a detection task.

The behavioral benefit of multiple pulses observed in the present study was surprisingly small. The difference in detectability between a single pulse and 31 pulses delivered at 100 Hz was ~0.3. Concerning temporal integration capacity, the gain in response probability of ~0.1 between rats' response rates to 31 versus 4 pulses when both were delivered at 100 Hz speaks for little impact of stimulus components arriving later than 40 ms after stimulus onset. Thus, repeated sensory evidence is accumulated in a highly sublinear way, as expressed by the attenuation of firing rates down to pulse frequencies of 10 Hz, in agreement with earlier findings in anesthetized animals (Chung et al., 2002; Garabedian et al., 2003; Khatri et al., 2004; Webber and Stanley, 2004). Sublinear accumulation is contrasted by our finding that longer integration times in fact would considerably improve detectability. The fact that the whisker system does not seem to make use of this to improve detectability leads us to the conclusion that it may not be designed to integrate weak signals over longer time periods for detection. This interpretation is in agreement with previous findings that vigorous responding of trigeminal whisker afferents to maintained deflection does not impact cortical firing (Pinto et al., 2000; Stüttgen and Schwarz, 2008) and also does not contribute to the animal's percept (Stüttgen et al., 2006). In fact, long integration time constants may be of harm for a system that strives to optimize discrimination, because long integration time windows blur the temporal aspect of spiking patterns. Behavioral observation of rats using their whiskers for navigation in darkness revealed that they touch obstructing objects just once before they significantly adapt their whisking pattern to take the presence of the detected object into consideration (Mitchinson et al., 2007). This observation supports the notion that object detection is typically accomplished using just a single contact. The neuronal basis for this behavior are extremely short integration windows yielding highest neurometric sensitivity (Stüttgen and Schwarz, 2008). Notably, a recent study using whiskered mobile robots (Fox et al., 2009) found that whisker vibration signals in the short periods (<50 ms) immediately following whisker-object contact onset and offset carry useful information about surface roughness.

The question arises whether the aforementioned processes apply for discrimination as well. Traditionally, it had been held that observers accumulate noisy information until sufficient to reach a decision and commit to a response, and integration times have originally been considered to be arbitrarily long [vision: Britten et al. (1992); touch: Hernández et al. (1997); for review, see Gold and Shadlen (2007)]. However, more recently, visual integration times have been shown to be optimally matched to behavior when limited to a few hundred milliseconds (Roitman and Shadlen, 2002; Kiani et al., 2008; Cohen and Newsome, 2009). Behavioral observation of whisking rats has revealed that tactile information is accumulated for rather short periods of time before committing to a choice. Individual touch durations are mostly <50 ms, reaching a maximum of 100 ms (von Heimendahl et al., 2007), with total palpation time (i.e., consecutive whisks) ranging from ~100–700 ms, being highly task-dependent (Carvell and Simons, 1995). It is intriguing to learn that during typical touch times as found in the study of von Heimendahl et al. (2007), temporal frequencies of <10–20 Hz cannot at all be represented in the vibrotactile signal entering the ascending tactile pathway. Does this mean that temporal frequencies below this range cannot be discriminated by rats? Not quite. The animals could change whisking speed to adjust the temporal frequency of incoming vibrotactile signals to a minimum of 20 Hz. Alternatively, it is certainly possible that the animals adapt touch times according to the spatiotemporal frequency at hand (Carvell and Simons, 1995).

In light of the behavioral constraints introduced by repetitive whisking discussed so far, it seems as if an integration time constant of ~5–8 ms (with significant integration up to 25 ms), as found in the present study, is compatible with the idea that vibrotactile signals arriving in barrel cortex are short enough to be readily integrated. Any two to three spikes arriving within a typical touch duration of 50 ms in barrel cortex would have a high chance to get integrated. This relates to a spike frequency of ~50 Hz, above which temporal integration would become significant. As whisker deflections often are responded by maximally one spike (Stüttgen et al., 2008; Jadhav et al., 2009), we expect that integration should play a role with pulsatile frequencies >50 Hz.

We hold it possible that the constraints of neuronal integration found in this study using a detection task may govern discrimination using active whisking as well. We hypothesize that the short time constant found in the present study acts to integrate the neuronal activity related to short strips of vibrotactile signals coming in with repetitive whisker strokes.

This view assigns a functional role for the strong suppression to repetitive pulsatile stimulation found here and in earlier work, which—at least partly—may be due to inhibitory processes lasting ~100 ms after a volley of cortical activation (Butovas and Schwarz, 2003; Butovas et al., 2006, Stüttgen and Schwarz, 2008; but see Chung et al., 2002). This response pattern may be tuned to the timing of chunks of vibrotactile signals [e.g., stick-slip events, instances of high acceleration in the vibrotactile signal brought about by interplay of surface and whisker mechanics (Arabzadeh et al., 2005; Wolfe et al., 2008; Ritt et al., 2008)] coming in at the rhythm of sequential whisker strokes. One study reported that, indeed, rats use repetitive whisking against a texture to reach a decision, mostly 1–3 consecutive whisks (von Heimendahl et al., 2007). Assuming a whisking frequency of ~7 Hz and touch times of 50 ms per single whisk (von Heimendahl et al., 2007) these strips of data would be integrated using the short time constant found in the present study and then separated by ~100 ms to the next touch time by suppression of signal flow in barrel cortex. In future studies it has to be worked out whether neuronal activity generated by active whisking (Fanselow and Nicolelis, 1999; Hentschke et al., 2006) may recruit memory systems, not available to our passively detecting rats, that in addition integrates information acquired across repetitive whisker strokes.

References

Arabzadeh E, Petersen RS, Diamond ME (2003) Encoding of whisker vibration by rat barrel cortex neurons: implications for texture discrimination. J Neurosci 23:9146–9154.

Arabzadeh E, Zorzin E, Diamond ME (2005) Neuronal encoding of texture in the whisker sensory pathway. PLoS Biol 3:e17.

Blackwell HR (1952) Studies of psychophysical methods for measuring visual thresholds. J Opt Soc Am 42:606–616.

Britten KH, Shadlen MN, Newsome WT, Movshon JA (1992) The analysis of visual motion: a comparison of neuronal and psychophysical performance. J Neurosci 12:4745–4765.

Butovas S, Schwarz C (2003) Spatiotemporal effects of microstimulation in rat neocortex: a parametric study using multielectrode recordings. J Neurophysiol 90:3024–3039.

Butovas S, Hormuzdi SG, Monyer H, Schwarz C (2006) Effects of electrically coupled inhibitory networks on local neuronal responses to intracortical microstimulation. J Neurophysiol 96:1227–1236.

Carvell GE, Simons DJ (1995) Task- and subject-related differences in sensorimotor behavior during active touch. Somatosens Mot Res 12:1–9.

Chung S, Li X, Nelson SB (2002) Short-term depression at thalamocortical synapses contributes to rapid adaptation of cortical sensory responses in vivo. Neuron 34:437–446.

Clark RE, Squire LR (1998) Classical conditioning and brain systems: the role of awareness. Science 280:77–81.

Cohen J (1992) A power primer. Psychological Bulletin 112: 155–159.

Cohen MR, Newsome WT (2009) Estimates of the contribution of single neurons to perception depend on timescale and noise correlation. J Neurosci 29:6635–6648.

Fanselow EE, Nicolelis MA (1999) Behavioral modulation of tactile responses in the rat somatosensory system. J Neurosci 19:7603–7616.

Fox CW, Mitchinson B, Pearson MJ, Pipe AG, Prescott TJ (2009) Contact type dependency of texture classification in a whiskered mobile robot. Auton Robot 26:223.

Galvez R, Weible AP, Disterhoft JF (2007) Cortical barrel lesions impair whisker-CS trace eyeblink conditioning. Learn Mem 14:94–100.

Garabedian CE, Jones SR, Merzenich MM, Dale A, Moore CI (2003) Band-pass response properties of rat SI neurons. J Neurophysiol 90:1379–1391.

Gescheider GA, Berryhill ME, Verrillo RT, Bolanowski SJ (1999) Vibrotactile temporal summation: probability summation or neural integration? Somatosens Mot Res 16:229–242.

Gold JI, Shadlen MN (2007) The neural basis of decision making. Annu Rev Neurosci 30:535–574.

Heil P, Neubauer H (2003) A unifying basis of auditory thresholds based on temporal summation. Proc Natl Acad Sci U S A 100:6151–6156.

Hentschke H, Haiss F, Schwarz C (2006) Central signals rapidly switch tactile processing in rat barrel cortex during whisker movements. Cereb Cortex 16:1142–1156.

Hermle T, Schwarz C, Bogdan M (2004) Employing ICA and SOM for spike sorting of multielectrode recordings from CNS. J Physiol Paris 98:349–356.

Hernández A, Salinas E, García R, Romo R (1997) Discrimination in the sense of flutter: New psychophysical measurements in monkeys. J Neurosci 17:6391–6400.

Hipp J, Arabzadeh E, Zorzin E, Conradt J, Kayser C, Diamond ME, König P (2006) Texture signals in whisker vibrations. J Neurophysiol 95:1792–1799.

Hutson KA, Masterton RB (1986) The sensory contribution of a single vibrissa's cortical barrel. J Neurophysiol 56:1196–1223.

Jadhav SP, Wolfe J, Feldman DE (2009) Sparse temporal coding of elementary tactile features during active whisker sensation. Nat Neurosci 12:792–800.

Jones LM, Lee S, Trageser JC, Simons DJ, Keller A (2004) Precise temporal responses in whisker trigeminal neurons. J Neurophysiol 92:665–668.

Khatri V, Hartings JA, Simons DJ (2004) Adaptation in thalamic barreloid and cortical barrel neurons to periodic whisker deflections varying in frequency and velocity. J Neurophysiol 92:3244–3254.

Kiani R, Hanks TD, Shadlen MN (2008) Bounded integration in parietal cortex underlies decisions even when viewing duration is dictated by the environment. J Neurosci 28:3017–3029.

Kline RB (2004) Beyond significance testing. Washington, DC: American Psychological Association.

Mitchinson B, Martin CJ, Grant RA, Prescott TJ (2007) Feedback control in active sensing: rat exploratory whisking is modulated by environmental contact. Proc Biol Sci 274:1035–1041.

Pinto DJ, Brumberg JC, Simons DJ (2000) Circuit dynamics and coding strategies in rodent somatosensory cortex. J Neurophysiol 83:1158–1166.

Ritt JT, Andermann ML, Moore CI (2008) Embodied information processing: vibrissa mechanics and texture features shape micromotions in actively sensing rats. Neuron 57:599–613.

Roitman JD, Shadlen MN (2002) Response of neurons in the lateral intraparietal area during a combined visual discrimination reaction time task. J Neurosci 22:9475–9489.

Salinas E, Hernandez A, Zainos A, Romo R (2000) Periodicity and firing rate as candidate neural codes for the frequency of vibrotactile stimuli. J Neurosci 20:5503–5515.

Sanchez-Jimenez A, Panetsos F, Murciano A (2009) Early frequency-dependent information processing and cortical control in the whisker pathway of the rat: electrophysiological study of brainstem nuclei principalis and interpolaris. Neuroscience 160:212–226.

Shadlen MN, Newsome WT (1996) Motion perception: seeing and deciding. Proc Natl Acad Sci U S A 93:628–633.

Stüttgen MC, Schwarz C (2008) Psychophysical and neurometric detection performance under stimulus uncertainty. Nat Neurosci 11:1091–1099.

Stüttgen MC, Rüter J, Schwarz C (2006) Two psychophysical channels of whisker deflection in rats align with two neuronal classes of primary afferents. J Neurosci 26:7933–7941.

Verrillo RT (1965) Temporal summation in vibrotactile sensitivity. J Acoust Soc Am 37:843–846.

von Heimendahl M, Itskov PM, Arabzadeh E, Diamond ME (2007) Neuronal Activity in Rat Barrel Cortex Underlying Texture Discrimination. PLoS Biol 5:e305.

Webber RM, Stanley GB (2004) Nonlinear encoding of tactile patterns in the barrel cortex. J Neurophysiol 91:2010–2022.

Wolfe J, Hill DN, Pahlavan S, Drew PJ, Kleinfeld D, Feldman DE (2008) Texture coding in the rat whisker system: slip-stick versus differential resonance. PLoS Biol 6:e215.

Zwislocki J (1960) Theory of temporal auditory summation. J Acoust Soc Am 32:1046–1060.